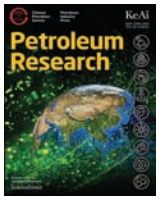
Petroleum Research 11 (2026) 50–62

Contents lists available at ScienceDirect

Petroleum Research

journal homepage: http://www.keaipublishing.com/en/journals/petroleum-research/



Full Length Article

Pseudo-pressure behavior in multilayered reservoir for single phase flow with permeability-pressure dependent



Jessica Lailla Ferreira Bittencourt Neto *, Sinésio Pesco, Abelardo Borges Barreto Júnior

Department of Mathematics, Pontifical Catholic University of Rio de Janeiro, Rio de Janeiro, 22451-900, Brazil

ARTICLE INFO

Article history:
Received 12 November 2024
Received in revised form
3 July 2025
Accepted 3 July 2025
Available online 9 July 2025

Keywords:
Pressure dependent permeability
Multilayered reservoir
Green's function
Pseudo-pressure

ABSTRACT

Mathematical techniques continue to become more advanced in developing more complex solutions in different fields, especially in oil reservoir simulation, where various physical parameters are still unknown. Studying different simulation cases that improve predictability is required to comprehend the wellbore behavior under production properly. This article proposes a new analysis method that utilizes the first-order asymptotic expansion method to address single-phase oil flow in multilayered reservoirs with permeability-pressure dependent and source terms. The classical techniques, like pseudo-pressure functions, although offering small linearization of the diffusivity equation, are found to be insufficient and thus require more efficient techniques like the Perturbation Method. The proposed model allows detailed analysis of different reservoir properties and pressure-dependent permeability curves, therefore allowing for more effective optimization and understanding of the flow behavior in complex geological conditions.

© 2025 Chinese Petroleum Society. Publishing services by Elsevier B.V. on behalf of KeAi Communications Co. Ltd. This is an open access article under the CC BY license (http://creativecommons.org/licenses/by/4.0/).

1. Introduction

Research efforts over the past years have improved the study of the effects of pressure-dependent rock properties such as compressibility, porosity, and permeability. Analytical and numerical approaches to identifying fluid characteristics have also been developed. Consequently, various solution methods have been proposed in theory, and numerous specific problems have been addressed using algorithms such as transient well testing and analytical reservoir modeling (Van Everdingen and Hurst, 1949). The line-source solution is a mathematical model commonly used in reservoir engineering to describe the pressure behavior around a well in a porous medium. Many studies are based on this formulation, dos Santos Sousa (2014) presented a line-source solution for gas well testing that incorporates wellbore storage and skin effects using the Green's functions approach. The study offers a semi-analytical framework that enhances the interpretation of pressure-transient data in gas reservoirs with complex well conditions. Ramey (1966) applied their results to the general fluid flow problem and proposed a new analytical solution to describe the pressure response of layered reservoirs with crossflow. Raghavan et al. (1972) investigated, through numerical methods, the impact of pressure-dependent rock and fluid properties on well flow tests. The study highlighted the importance of incorporating nonlinear effects when interpreting transient pressure data in deformable formations.

The literature shows that the problems have become more complex over the years, requiring different formulations, assumptions, and mathematical models that could get close to accurate representations of a reservoir's geometry and physical properties (Fernandes et al., 2025; Lee and Wattenbarger, 2016; Miranda et al., 2016; Wang, 2023). Throughout evolution, estimating reservoir parameters gained prominence in works related to the production area. Duong (1989) introduced a novel set of type curves for well-test analysis in homogeneous reservoirs, accounting for wellbore storage and skin effects. These new type curves help mitigate the issue of non-uniqueness in pressure-transient type-curve matching, enable more effective identification of flow regimes, and provide increased confidence in the analysis results. On the other hand, studies related to the interpretation of graphs of the response of the pressure behavior were analyzed Bourdet (1985). The analysis of layered reservoir

* Corresponding author.
E-mail addresses: jessicabittencourtn@gmail.com (J. Lailla Ferreira Bittencourt Neto), sinesio@puc-rio.br (S. Pesco), abelardo-puc@gmail.com (A. Borges Barreto Júnior).

Peer review under the responsibility of Editorial Office of Petroleum Research.

https://doi.org/10.1016/j.ptlrs.2025.07.002
2096-2495/© 2025 Chinese Petroleum Society. Publishing services by Elsevier B.V. on behalf of KeAi Communications Co. Ltd. This is an open access article under the CC BY license (http://creativecommons.org/licenses/by/4.0/).

Nomenclature

Symbol	Variable NameUnit (Brazil)SI Unit
α_p	Adequacy constant for pressure
α_t	Adequacy constant for time
v_j	Darcy velocity in layer jm/day$m$/s
δ	Dirac delta function1/(variable unit)1/(variable unit)
ρ	Density$kg/m^3kg/m^3$
H_{Dj}	Dimensionless diffusivity coefficient of layer j
q_{Dj}	Dimensionless flow rate of layer j
w_{Dj}	Dimensionless hydraulic deviation of layer j
G_{Dj}	Dimensionless Green's function of layer j
k_{Dj}	Dimensionless permeability function of layer j
p_D	Dimensionless pressure
p_{Dj}	Dimensionless pressure of layer j
m_D	Dimensionless pseudo-pressure
m_{Dj}	Dimensionless pseudo-pressure of layer j
r_D	Dimensionless radius
r_{0D}	Dimensionless source radius
t_{0D}	Dimensionless source time
f_{Dj}	Dimensionless source function
r_{0D}	Dimensionless source radius
t_D	Dimensionless time
m_{wD}	Dimensionless well bottom-hole pseudo-pressure
k_{eq}	Equivalent permeabilitymDm^2
c_f	Fluid compressibility$(\mathrm{kgf/cm^2})^{-1}$1/Pa
q_j	Flow rate of layer jm^3/daym^3/s
p_i	Initial reservoir pressurePaPa
C_j	Mobility ratio of layer j
μ	Oil viscositycPPa ·s
$k_j(p)$	Permeability function of layer $jmDm^2$
	Perturbative coefficient
	Porosity
p_j	Pressure in layer $j$kgf/cm^{2}Pa
r	Radiusmm
q_{ref}	Reference flow ratem^3/daym^3/s
c_r	Rock compressibility$(\mathrm{kgf/cm^2})^{-1}$1/Pa
h_j	Thickness of layer jmm
t	Time$days$
c_t	Total compressibility$(\mathrm{kgf/cm^2})^{-1}$1/Pa
h_t	Total reservoir thickness (sum of the thicknesses of all layers)mm
p_{wD}	Well bottom-hole pressurekgf/cm^{2}Pa
q	Well flow ratem^3/daym^3/s
r_w	Well radiusmm

behavior through pressure and pressure derivative responses provides valuable insights into reservoir dynamics. This approach clearly defines the limits of applicability for homogeneous and double-porosity solutions when interpreting tests in layered formations. A novel model has been applied to an actual field case, demonstrating its ability to achieve a strong match where conventional solutions fail. In addition to estimating standard well and reservoir parameters such as the total permeability-thickness product, skin factor, and wellbore storage coefficient, the model offers quantitative information on the storativity and permeability of contrasting layers, enhancing the understanding of complex reservoir systems.

The permeability of reservoir is an important property because it allows us to gain markable insights into a fluid's flow. However, measuring the permeability of a reservoir is costly and, in many cases, unfeasible. For this reason, it is common to observe in the literature the study of the behavior of the pressure response for different scenarios for the value of this variable and/or permeability estimation values (Raghavan, 1993). Research topics involving the use of the physical properties of an oil reservoir as a function of pressure have been timidly explored over the last few years. Civan (2016) shows that the study of permeability as a function of pressure becomes a crucial topic for improving reservoir management and optimizing extraction processes. With this, it is possible to develop more accurate reservoir simulation models that resemble the reality of nature. It also improves recovery factors by adjusting oil recovery strategies, mitigating risks, and obtaining insights for the management of unconventional reservoirs, where traditional models may not be applicable. The interpretation of the pressure-dependent permeability as a variable in the mathematical problem applied to different reservoir types, as discussed by Chen et al. (2006), ensures more reliable predictions about pressure production behavior, enabling more efficient and sustainable resource extraction. The hydraulic diffusivity equation is a nonlinear equation that governs flow in porous media. The nonlinearity of this equation aroused the need to disseminate linearization methods. A pseudo-pressure method does not fully linearize the problem, requiring alternative methods to solve the nonlinear portion, as highlighted by Gringarten and Ramey (1973).

Green's Functions are mathematical tools that can solve many problems, including flow in porous media. Applied to modeling petroleum reservoirs, Green's Functions allow the linearization of part of the differential equation that governs fluid flow in porous media. The analytical solution obtained for the problem with this method can be expressed as an integral that includes the initial and boundary conditions. Several works in the literature present a formulation using Green's functions. Duff (2001) presents applications of using Green's functions in different mathematical problems that can be applied to engineering, physics, and other scenarios. This book guided different authors to apply this methodology to approximate solutions for reservoir flow.

As part of developing models for multilayer reservoirs, Singh and Whitson (2010) investigated systems in which individual layers may exhibit significant variations in permeability and composition. These layers can be either hydraulically connected or isolated, and their behavior can be effectively described using pseudopressure formulations. The pseudopressure method is beneficial in well modeling for coarse-grid reservoir simulations with relatively large areal grid blocks, as it enables the accurate representation of near-well condensate blockage effects without the need for local grid refinement. Significant progress has been made in developing analytical solutions for gas flow in reservoirs by applying Green's Functions and advanced mathematical techniques. Barreto (2011) presented a general solution for vertical gas wells near sealing faults using an asymptotic expansion coupled with Green's Functions, demonstrating high accuracy compared to finite difference models. Expanding on this, Barreto et al. (2012) introduced a pseudo-pressure-based solution to analyze gas flow in fractured porous media, incorporating a corrective first-order term in the series expansion to achieve excellent agreement with numerical simulators. Later, Barreto et al. (2013) advanced these methods by addressing the nonlinear effects of the viscosity-

compressibility product, developing a perturbative solution for variable rate tests in infinite gas reservoirs. This approach provided precise approximations for engineering applications, as validated against synthetic datasets and commercial simulators. Further refinements were made by Sousa et al. (2015, 2016), who considered finite well radius (FWR) boundary conditions and storage and skin effects in homogeneous reservoirs, presenting solutions that accurately matched numerical simulators at long times. Additionally, Neto (2019) extended the application of Green's Functions and the Perturbative Method to heterogeneous reservoirs composed of two homogeneous permeability regions, offering valuable insights into composite systems. Collectively, these contributions underscore the versatility and robustness of Green's Functions in modeling complex gas flow scenarios, providing powerful tools for reservoir engineering analysis.

The studies referring to the gas flow were mainly explored. Thus, several analytical studies have been developed and the main objective is to solve the Nonlinear Hydraulic Differential Equation for oil flow in a reservoir considering the pressure sensitive to permeability from a perturbative-integral-differential model. The general methodology combines a first-order asymptotic series expansion, Green's functions (GF), and a second-type Volterra integral-differential formulation (Fernandes et al., 2023a,b). The model validation is carried out by comparing the developed solution with a numerical simulator of porous oil flow. The models presented above are significant contributions because they allow a better understanding of pseudo-pressure behavior by considering fluid properties that are a function of pressure. The extension of these works to more complex problems brings mathematical modeling closer to the physical reality of reservoirs, in which exploration must be carefully studied for better industry decision-making.

The study of pressure behavior is essential for operational efficiency and economic success in the oil industry, especially when understanding fluid flow in porous media. While many models assume constant reservoir permeability, it is well-known that permeability can vary throughout a reservoir. To address this variability in oil extraction, this work utilizes the hypothesis of pressure-dependent permeability, providing a more realistic model for predicting single-phase oil flow. This approach enhances the accuracy of flow responses and contributes to the optimization of oil extraction.

The paper proposes an approximate solution for oil flow in multilayer reservoirs, considering permeability-dependent pseudo-pressure, offering a more realistic framework for reservoir prediction and optimization. Then, the formulation for an n-layer reservoir is presented, and the results obtained for the formulations using different reservoir properties are discussed.

2. Problem statement

This section presents a formulation for a multilayered reservoir with single-phase oil flow. Starting from the single-layer formulation proposed by Fernandes (2022), Neto (2019), Barreto (2011), and Barreto et al. (2013), we developed a formulation that describes the permeability-dependent pseudo-pressure behavior for oil flow for a n-layer reservoir. Although the formulations of these works are focused on gas flow, we adapted some assumptions and definitions for our purpose.

2.1. Mathematical model

Bittencourt Neto et al. (2020) proposed a formulation for single-phase oil flow in a multilayered reservoir with constant permeability. The geometric configuration of the n-layer reservoir resembles the system studied in this work, represented by Fig. 1. Elements of this formulation can be adapted to the objective of our mathematical model, which involves incorporating a permeability-pressure function. This adaptation allows for a more dynamic representation of reservoir behavior, providing greater insight into the interactions between pressure and permeability in complex reservoir systems.

Some assumptions about the porous medium are necessary to simplify the mathematical formulation:

- Constant initial permeability in all three directions;
- Constant flow-rate;
- Isothermal, single-phase and radial flow;
- Fluid with low compressibility
- Infinite and isotropic reservoir per layer;
- Negligible gravitational effects
- Storage effects and formation damage in the producing well will be disregarded;
- There is no communication between layers except in the wellbore.

Therefore, for each layer j, the following initial and boundary conditions are defined. The initial condition corresponds to the pressure distribution in each layer at the initial time, reflecting the reservoir's initial state.

$$p_j(r, t=0) = p_i \tag{1}$$

The Internal Boundary Condition is relative to the constant flow rate in the well at each layer.

$$q_j(r,t) = \frac{2\pi h_j}{\mu}\left(k_j(p_j(r,t))r\frac{\partial p_j(r,t)}{\partial r}\right)_{r=r_w} \tag{2}$$

The External Boundary Condition is relative to the infinite reservoir.

$$\lim_{r\to\infty} p_j(r,t) = p_i \tag{3}$$

Starting from the Continuity Equation for a fluid:

$$\frac{1}{r}\frac{\partial}{\partial r}(r\rho v_j) = -\frac{\partial}{\partial t}(\phi\rho) \tag{4}$$

Where by Darcy's Law:

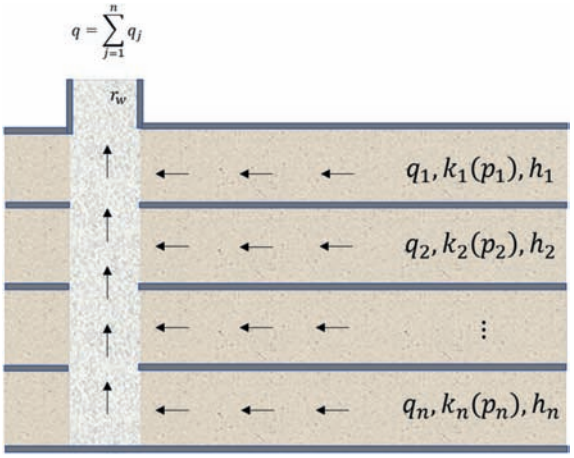


Fig. 1. Reservoir model with multiple layers.

$$v_j = -\frac{k_j(p_j(r,t))}{\mu}\frac{\partial p_j(r,t)}{\partial r} \tag{5}$$

Therefore, replacing (5) in (4):

$$\frac{1}{r}\frac{\partial}{\partial r}\left(\rho\frac{k_j(p_j(r,t))}{\mu}r\frac{\partial p_j(r,t)}{\partial r}\right) = -\frac{\partial}{\partial t}(\phi\rho) \tag{6}$$

Applying the Chain Rule to the right of the previous equation:

$$\frac{\partial}{\partial t}(\phi\rho) = \phi\frac{\partial\rho}{\partial t} + \rho_j\frac{\partial\phi_j}{\partial t} \tag{7}$$

Considering the compressibilities $c_f = \frac{1}{\rho}\frac{\partial\rho}{\partial p_j}$ e $c_r = \frac{1}{\phi}\frac{\partial\phi}{\partial p_j}$ we have:

$$\frac{\partial\rho}{\partial t} = c_f\rho\frac{\partial p_j(r,t)}{\partial t} \tag{8}$$

and

$$\frac{\partial\phi}{\partial t} = c_r\phi\frac{\partial p_j(r,t)}{\partial t} \tag{9}$$

Replacing (7), (8) and (9) in (6):

$$\frac{1}{r}\frac{\partial}{\partial r}\left(\rho\frac{k_j(p_j(r,t))}{\mu}r\frac{\partial p_j(r,t)}{\partial r}\right) = -\phi\rho c_t\frac{\partial p_j(r,t)}{\partial t} \tag{10}$$

where $c_t = c_f + c_r$.

Considering ρ and μ are constant, the previous equation becomes as follows:

$$\frac{1}{r}\frac{\partial}{\partial r}\left(rk_j(p_j(r,t))\frac{\partial p_j(r,t)}{\partial r}\right) = -\phi\mu c_t\frac{\partial p_j(r,t)}{\partial t} \tag{11}$$

Considering the definition for the pressure variation like $\Delta p_j(r, t) = p_i - p_j(r, t)$, the problem can be rewritten. On the other hand, the hypotheses assumed at the beginning of this section allow us to write an initial condition and the following boundary conditions in terms of $\Delta p_j(r, t)$:

Partial Diffential Equation (PDE):

$$\frac{1}{r}\frac{\partial}{\partial r}\left(rk_j(p_j(r,t))\frac{\partial\Delta p_j(r,t)}{\partial r}\right) = -\phi\mu c_t\frac{\partial\Delta p_j(r,t)}{\partial t} \tag{12}$$

The Initial Condition (IC) is relative to the reservoir being in equilibrium at the initial time.

$$\Delta p_j(r, t=0) = 0 \tag{13}$$

The Internal Boundary Condition (IBC) is relative to the constant oil flow-rate in the well.

$$q_j(r_w,t) = -\frac{2\pi h_j}{\mu}\left(rk_j(p_j(r,t))\frac{\partial\Delta p_j(r,t)}{\partial r}\right)|_{r=r_w} \tag{14}$$

The External Boundary Condition (EBC) is relative to the infinite reservoir.

$$\lim_{r\to\infty}\Delta p_j(r,t) = 0 \tag{15}$$

Furthermore, we must consider the Coupling Conditions between layers (CCL). Therefore, we must consider the following equations:

CCL-pressure

$$\Delta p_1(r,t) = \Delta p_2(r,t) = \ldots = \Delta p_n(r,t) \tag{16}$$

CCL - flow-rate

$$q = q_1(r_w,t) + q_2(r_w,t) + \cdots + q_n(r_w,t) \tag{17}$$

2.2. The pseudo-pressure model

The pseudo-pressure function ($m_j(p_j(r, t))$) that will be interesting to our model purpose is defined as follows:

$$m_j(p_j(r,t)) = \int_{p_B}^{p_j(r,t)} k_j(x)dx \tag{18}$$

where p_B is a reference pressure.

Thus, the variation of the pseudo-pressure ($\Delta m_j(p_j(r, t))$) is given by:

$$\Delta m_j(p_j(r,t)) = m_j(p_i) - m_j(p_j(r,t)) = \int_{p_j(r,t)}^{p_i} k_j(x)dx \tag{19}$$

To facilitate the reader's understanding, we will adopt the pseudo-pressure notation $\Delta m_j(p_j(r, t)) = \Delta m_j(r, t)$. So, starting from the definition of Δm_j:

$$\frac{\partial\Delta m_j(r,t)}{\partial r} = -\frac{k_j(p_j(r,t))}{\mu}\frac{\partial p_j(r,t)}{\partial r} = \frac{k_j(p_j(r,t))}{\mu}\frac{\partial\Delta p_j(r,t)}{\partial r} \tag{20}$$

and

$$\frac{\partial\Delta m_j(r,t)}{\partial t} = -\frac{k_j(p_j(r,t))}{\mu}\frac{\partial p_j(r,t)}{\partial t} = \frac{k_j(p_j(r,t))}{\mu}\frac{\partial\Delta p_j(r,t)}{\partial t} \tag{21}$$

So, replacing (20) and (21) in (11) the Diffusivity Equation is obtained as a function of pseudo-pressure ($\Delta m_j(p_j)$):

$$\frac{1}{r}\frac{\partial}{\partial r}\left(r\frac{\partial\Delta m_j(r,t)}{\partial r}\right) = \frac{\phi c_t\mu}{k_j(p_j(r,t))}\left(\frac{\partial\Delta m_j(r,t)}{\partial t}\right) \tag{22}$$

with the following boundary conditions in terms of $\Delta m_j(r, t)$:

Initial Condition:

$$\Delta m_j(r, t=0) = m_j(p_i) - m_j(r, t=0) = 0 \tag{23}$$

Internal Boundary Condition:

$$q_j(r_w,t) = -\frac{2\pi h_j}{\mu}\left(r\frac{\partial\Delta m_j(r,t)}{\partial r}\right)_{r=r_w} \tag{24}$$

External Boundary Condition:

$$\lim_{r\to\infty}\Delta m_j(r,t) = 0 \tag{25}$$

Considering an one-layer equivalente reservoir as a reference, the dimensionless variables for radius and time will be defined as:

$$r_D = \frac{r}{r_w} \tag{26}$$

and

$$t_D = \frac{k_{eq}(p_i)}{\phi\mu c_t r_w^2}t \tag{27}$$

where $k_{eq}(p_i)$ is the initial equivalent permeability given by:

$$k_{eq}(p_i) = \frac{k_1(p_i)h_1 + k_2(p_i)h_2 + \cdots + k_n(p_i)h_n}{h_1 + h_2 + \cdots + h_n} \tag{28}$$

The spatial and time adimensional derivatives are:

$$\frac{\partial r_D}{\partial r} = \frac{1}{r_w} \tag{29}$$

and

$$\frac{\partial t_D}{\partial t} = \frac{k_{eq}(p_i)}{\phi\mu c_t r_w^2} \tag{30}$$

With that, the partial derivatives of the pseudo-pressure variation can be written as:

$$\frac{\partial \Delta m_j(r,t)}{\partial r} = \frac{\partial \Delta m_j(r_D,t_D)}{\partial r_D}\frac{\partial r_D}{\partial r} = \frac{1}{r_w}\frac{\partial \Delta m_j(r_D,t_D)}{\partial r_D} \tag{31}$$

and

$$\frac{\partial \Delta m_j(r,t)}{\partial t} = \frac{\partial \Delta m_j(p_j(r_D,t_D))}{\partial t_D}\frac{\partial t_D}{\partial t} = \frac{k_{eq}(p_i)}{\phi\mu c_t r_w^2}\frac{\partial \Delta m_j(p_j(r_D,t_D))}{\partial t_D} \tag{32}$$

Replacing (31) and (32) in (22):

$$\frac{1}{r_D}\frac{\partial}{\partial r_D}\left(r_D\frac{\partial \Delta m_j(r_D,t_D)}{\partial r_D}\right) = \frac{k_{eq}(p_i)}{k_j(p_j)}\frac{\partial \Delta m_j(r_D,t_D)}{\partial t_D} \tag{33}$$

Defining the diffusivity coefficient $\kappa_{D_j}(p_j(r_D,t_D)) = \frac{k_j(p_j(r_D,t_D))}{k_{eq}(p_i)}$ one get that:

$$\frac{1}{r_D}\frac{\partial}{\partial r_D}\left(r_D\frac{\partial \Delta m_j(p_j(r_D,t_D))}{\partial r_D}\right) = \frac{1}{\kappa_{D_j}(r_D,t_D)}\frac{\partial \Delta m_j(p_j(r_D,t_D))}{\partial t_D} \tag{34}$$

Therefore, using the previous definitions, the boundary conditions can be written as follow:

Initial Condition:

$$\Delta m_j(r_D, t_D = 0) = 0 \tag{35}$$

Internal Boundary Condition:

$$q_j = -\frac{2\pi h_j}{\mu}\left(r_D\frac{\partial \Delta m_j(r_D,t_D)}{\partial r_D}\right)_{r_D=1} \tag{36}$$

External Boundary Condition:

$$\lim_{r\to\infty}\Delta m_j(r_D,t_D) = 0 \tag{37}$$

Defining the dimensionless pseudo-pressure $m_{D_j}(r_D,t_D)$ such that:

$$m_{D_j}(r_D,t_D) = \frac{2\pi h_t}{q\mu}\Delta m_j(r_D,t_D) \tag{38}$$

So,

$$\frac{\partial m_{D_j}(r_D,t_D)}{\partial r_D} = \frac{2\pi h_t}{q\mu}\frac{\partial \Delta m(p_j(r_D,t_D))}{\partial r_D} \tag{39}$$

and

$$\frac{\partial m_{D_j}(r_D,t_D)}{\partial t_D} = \frac{2\pi h_t}{q\mu}\frac{\partial \Delta m(p_j(r_D,t_D))}{\partial t_D} \tag{40}$$

Thus, replacing (39) and (40) in the IBC (36):

$$\left(r_D\frac{\partial m_{D_j}(r_D,t_D)}{\partial r_D}\right)_{r_D=1} = -\frac{q_j h_t}{q h_j} = -C_j \tag{41}$$

Finally, the equations can be written more compactly by writing the proposed problem with dimensionless variables as follow:

PDE:

$$\frac{1}{r_D}\frac{\partial}{\partial r_D}\left(r_D\frac{\partial m_{D_j}(r_D,t_D)}{\partial r_D}\right) = \frac{1}{\kappa_{D_1}}\frac{\partial m_{D_j}(r_D,t_D)}{\partial t_D} \tag{42}$$

Initial Condition:

$$m_{D_j}(r_D, t_D = 0) = 0 \tag{43}$$

Internal Boundary Condition:

$$\left(r_D\frac{\partial m_{D_j}(r_D,t_D)}{\partial r_D}\right)_{r_D=1} = -\frac{q_j h_t}{q h_j} \tag{44}$$

External Boundary Condition:

$$\lim_{r\to\infty} m_{D_j}(r_D,t_D) = 0 \tag{45}$$

In the model presented, the permeability curve depends on pressure, and the pseudo pressure is also associated with a pressure value associated with permeability, so we will adopt the notation $k_D(p_j) = k_{D_j}(m_{D_j})$.

Defining the dimensionless diffusivity coefficient $H_{D_j}(m_{D_j}) = \frac{1}{k_{D_j}(m_{D_j})}$ we have the PDE without source term:

$$\frac{1}{r_D}\frac{\partial}{\partial r_D}\left(r_D\frac{\partial m_{D_j}(r_D,t_D)}{\partial r_D}\right) = H_{D_j}(m_{D_j})\frac{\partial m_{D_j}(r_D,t_D)}{\partial t_D} \tag{46}$$

Initial Condition

$$m_{D_j}(r_D, t_D = 0) = 0 \tag{47}$$

Internal Boundary Condition:

$$\left(r_D\frac{\partial m_{D_j}(r_D,t_D)}{\partial r_D}\right)_{r_D=1} = -\frac{q_j h_1}{q_1 h_j} = C_j \tag{48}$$

External Boundary Condition:

$$\lim_{r\to\infty} m_{D_j}(r_D,t_D) = 0 \tag{49}$$

Considering now the PDE with source term can be written as:

$$\frac{1}{r_D}\frac{\partial}{\partial r_D}\left(r_D\frac{\partial m_{D_j}(r_D,t_D)}{\partial r_D}\right) - H_{D_j}(m_{D_j})\frac{\partial m_{D_j}(r_D,t_D)}{\partial t_D} = f_{D_j}(r_D,t_D) \tag{50}$$

The hydraulic deviation $w_{D_j}(m_{D_j})$ will be defined by:

$$w_{D_j}(m_{D_j}) = H_{D_j}(m_{D_j}) - 1 \tag{51}$$

Thereby:

$$\frac{1}{r_D}\frac{\partial}{\partial r_D}\left(r_D\frac{\partial m_{D_j}(r_D,t_D)}{\partial r_D}\right) - \frac{\partial m_{D_j}(r_D,t_D)}{\partial t_D} = w_{D_j}(m_{D_j})\frac{\partial m_{D_j}(r_D,t_D)}{\partial t_D} + f_{D_j}(r_D,t_D) \tag{52}$$

2.3. Green's function

The Green's function associated with our problem depends on the infinity radial geometry. In the literature, this method was applied in similar cases of geometry (Barreto, 2011; dos Santos

Sousa, 2014; Fernandes, 2022; Fernandes et al., 2023; Fernandes et al., 2025). Volterra's integral-differential equation finds the solution for this model. It can be found after mathematics manipulations of the spatial integrating and temporal integration of the proposed problem equation and associated Green's problem resulting in the follow solution:

$$m_{D_j}(r_D,t_D)=\frac{-2\pi}{C_j}\int_0^{\infty}\int_0^{t_D}\Big[f_{D_j}(r'_D,t'_D)+w_{D_j}(p_{D_j})\times\Big]r'_D G_{D_j}(r_D,r'_D,t_D,t'_D)dt'_D dr'_D \tag{53}$$

where Green's function (G_{D_j}) is of the form:

$$G_{D_j}(r_D,r'_D,t_D,t'_D)=\frac{exp\left(-\frac{(r_D-r'_D)^2}{4(t_D-t'_D)}\right)}{4\pi(t_D-t'_D)}I_0\left(\frac{r_D r'_D}{2(t_D-t'_D)}\right) \tag{54}$$

The source function f_{D_j} can be defined as:

$$f_{D_j}(r_D,t_D)=-2\pi q_{D_j}(t_D)\delta(r_D-r'_D) \tag{55}$$

where δ is the Dirac delta function and q_{D_j} represents the dimensionless flow-rate:

$$q_{D_j}(t_D)=\frac{q_j(t)}{q_{sc}} \tag{56}$$

Replacing (54) and (55) in (53) after apply the dirac delta property:

$$m_{D_j}(r_D,t_D)=\frac{1}{C_j}p_{D_j}(r_D,t_D)-\frac{2\pi}{C_j}\int_0^{\infty}\times\int_0^{t_D}r'_D w_{D_j}(p_{D_j})\frac{\partial m_{D_j}(r'_D,t'_D)}{\partial t_D}G_{D_j}(r_D,r'_D,t_D,t'_D)dt'_D dr'_D \tag{57}$$

where $p_{D_j}(r_D,t_D)$ is represented by the well known Line-Source Solution:

$$p_{D_j}(r_D,t_D)=-\frac{1}{2}Ei\left(\frac{-r_D^2}{4t_D}\right) \tag{58}$$

2.4. Pertubation and power method

One of the great potentialities of the Perturbation Method is its ability to approach non-linear differential equations through a succession of linear equations, which are more uncomplicated to solve. In this methodology, the diffusivity equation with pressure-dependent permeability (Eq. (52)) is perturbed by introducing variable ε by multiplying the factor responsible for the nonlinearity.

$$\frac{1}{r_D}\frac{\partial}{\partial r_D}\left(r_D\frac{\partial m_{D_j}(r_D,t_D)}{\partial r_D}\right)-\frac{\partial m_{D_j}(r_D,t_D)}{\partial t_D}=\epsilon w_{D_j}(m_{D_j})\frac{\partial m_{D_j}(r_D,t_D)}{\partial t_D}+f_{D_j}(r_D,t_D) \tag{59}$$

Considering that the pseudo-pressure can be represented by an asymptotic expansion of powers of ε:

$$m_{D_j}(r_D,t_D)=\sum_{k=0}^{\infty}\epsilon^k m_{D_j}^{(k)}(r_D,t_D) \tag{60}$$

Replacing (60) in (59) and rearranging the terms according to the powers of ε:

$$\epsilon^0\left[\frac{1}{r_D}\frac{\partial}{\partial r_D}\left(r_D\frac{\partial m_{D_j}^{(0)}(r_D,t_D)}{\partial r_D}\right)-\frac{\partial m_{D_j}^{(0)}(r_D,t_D)}{\partial t_D}-f_{D_j}(r_D,t_D)\right]+\cdots+\epsilon^k\left[\frac{1}{r_D}\frac{\partial}{\partial r_D}\left(r_D\frac{\partial m_{D_j}^{(k)}(r_D,t_D)}{\partial r_D}\right)-\frac{\partial m_{D_j}^{(k)}(r_D,t_D)}{\partial t_D}-w_{D_j}(m_{D_j}^{(k-1)})\frac{\partial m_{D_j}^{(k-1)}(r_D,t_D)}{\partial t_D}\right]+\ldots=0 \tag{61}$$

The following definition was adopted to simplify the visualization of the equations terms:

$$w_{D_j}\left(m_{D_j}^{(k-1)}\right)=w_{D_j}\left(\sum_{i=0}^{k-1}\epsilon^i m_{D_j}^{(i)}(r_D,t_D)\right) \tag{62}$$

So the problem becomes a system of the form:
Order 0:

$$\text{PDE: }\frac{1}{r_D}\frac{\partial}{\partial r_D}\left(r_D\frac{\partial m_{D_j}^{(0)}(r_D,t_D)}{\partial r_D}\right)-\frac{\partial m_{D_j}^{(0)}(r_D,t_D)}{\partial t_D}-f_{D_j}(r_D,t_D)=0; \tag{63}$$

$$\text{IC: }m_{D_j}^{(0)}(r_D,t_D)=0; \tag{64}$$

$$\text{EBC: }\lim_{r_D\to\infty}m_{D_j}^{(0)}(r_D,t_D)=0; \tag{65}$$

Order $k\geq 1$:

$$\text{PDE: }\frac{1}{r_D}\frac{\partial}{\partial r_D}\left(r_D\frac{\partial m_{D_j}^{(k)}(r_D,t_D)}{\partial r_D}\right)-\frac{\partial m_{D_j}^{(k)}(r_D,t_D)}{\partial t_D}-w_{D_j}(m_{D_j}^{(k-1)})\frac{\partial m_{D_j}^{(k-1)}(r_D,t_D)}{\partial t_D}=0; \tag{66}$$

$$\text{IC: }m_{D_j}^{(k)}(r_D,t_D)=0; \tag{67}$$

$$\text{EBC: }\lim_{r_D\to\infty}m_{D_j}^{(k)}(r_D,t_D)=0; \tag{68}$$

Considering the Volterra's integro-differential equation:

$$m_{D_j}^{(0)}(r_D,t_D)=\frac{1}{C_j}p_{D_j}(t_D) \tag{69}$$

and

$$m_{D_j}^{(k)}(r_D,t_D)=\int_0^{\infty}\times\int_0^{t_D}w_{D_j}(m_{D_j}^{(k-1)})\frac{\partial m_{D_j}^{(k-1)}}{\partial t_D}G_D(r_D,r'_D,t_D,t'_D)dt'_D dr'_D \tag{70}$$

From the 1st order problem, the calculation of the solutions depends on the solution of the previous order problem. Therefore, like in Barreto (2011) and Fernandes (2022), we considered that the truncation in the term of order one is sufficient. Order 0:

$$PDE: \frac{1}{r_D}\frac{\partial}{\partial r_D}\left(r_D\frac{\partial m_{D_j}^{(0)}(r_D,t_D)}{\partial r_D}\right)-\frac{\partial m_{D_j}^{(0)}(r_D,t_D)}{\partial t_D}-f_{D_j}(r_D,t_D)=0; \tag{71}$$

$$IC: m_{D_j}^{(0)}(r_D,t_D)=0; \tag{72}$$

$$EBC: \lim_{r_D\to\infty} m_{D_j}^{(0)}(r_D,t_D)=0; \tag{73}$$

Order 1:

$$PDE: \frac{1}{r_D}\frac{\partial}{\partial r_D}\left(r_D\frac{\partial m_{D_j}^{(1)}(r_D,t_D)}{\partial r_D}\right)-\frac{\partial m_{D_j}^{(1)}(r_D,t_D)}{\partial t_D} - w_{D_j}(p_{D_j})\frac{\partial m_{D_j}^{(1)}(r_D,t_D)}{\partial t_D} = 0; \tag{74}$$

$$IC: m_{D_j}^{(1)}(r_D,t_D)=0; \tag{75}$$

$$EBC: \lim_{r_D\to\infty} m_{D_j}^{(1)}(r_D,t_D)=0; \tag{76}$$

where for each system of equation the solution is given by:

$$m_{D_j}^{(0)}(r_D,t_D)=\frac{1}{C_j}p_{D_j}(r_D,t_D) \tag{77}$$

and

$$m_{D_j}^{(1)}(r_D,t_D)=-\frac{2\pi}{C_j}\int_0^{\infty}\times\int_0^{t_D} r'_D w_{D_j}(p_{D_j})\frac{\partial p_{D_j}}{\partial t_D}G_D(r_D,r'_D,t_D,t'_D)dt'_D dr'_D \tag{78}$$

Note that for $\varepsilon=1$ we have the original problem. Therefore, the solution for m_{D_j} is given by:

$$m_{D_j}(r_D,t_D)=m_{D_j}^{(0)}(r_D,t_D)+m_{D_j}^{(1)}(r_D,t_D) = p_{D_j}(r_D,t_D)+m_{D_j}^{(1)}(r_D,t_D) \tag{79}$$

2.5. Problem solution

We aim to find a solution for the pseudo-pressure behavior in the wellbore. Until here, we use different mathematical tools to solve each layer problem. Now we will couple these solutions to obtain a single answer for the pseudo-pressure behavior in the well. So, knowing the pressure solution for each layer (Eq. (79)), we have the following coupling conditions in the well:

Pseudo-pressure Coupling Condition:

$$m_{D_1}(r_D=1,t_D)=m_{D_2}(r_D=1,t_D)=\ldots=m_{D_n}(r_D=1,t_D) \tag{80}$$

Flow-rate Coupling Condition:

$$q_1(r_D=1,t_D)+q_2(r_D=1,t_D)+\cdots+q_n(r_D=1,t_D)=1 \tag{81}$$

Furthermore, we know that the single-phase oil solution in the well in multilayer reservoirs is the same in each layer, i.e.

$$p_D(t_D)=p_{D_1}(r_D=1,t_D)=p_{D_2}(r_D=1,t_D)=\ldots=p_{D_n}(r_D=1,t_D) \tag{82}$$

Replacing C_j definition at Eqs. (77) and (78):

$$m_{D_j}(r_D,t_D)=\frac{h_j}{q_{D_j}h_T}p_D(t_D)-\frac{2\pi h_j}{q_{D_j}h_T}\int_0^{\infty}\int_0^{t_D} r'_D w_{D_j}(p_{D_j})\frac{\partial p_{D_j}(r'_D,t'_D)}{\partial t_D}G_{D_j}(r_D,r'_D,t_D,t'_D),\ dt'_D dr'_D \tag{83}$$

Therefore, the equation can be rewritten as:

$$q_{D_j}=\frac{h_j}{h_T m_{D_j}(r_D,t_D)}p_D(t_D)-2\pi\frac{h_j}{h_T m_{D_j}(r_D,t_D)}\int_0^{\infty}\times\int_0^{t_D} r'_D w_{D_j}(p_{D_j})\frac{\partial p_{D_j}(r'_D,t'_D)}{\partial t_D}G_{D_j}(r_D,r'_D,t_D,t'_D),\ dt'_D dr'_D \tag{84}$$

Replacing Eq. (84) in the Flow-rate Coupling Condition (Eq. (81)):

$$\sum_{i=1}^{n}\frac{h_j}{h_T m_{D_j}(r_D,t_D)}\left(p_D(t_D)-2\pi\int_0^{\infty}\times\int_0^{t_D} r'_D w_{D_j}(p_{D_j})\frac{\partial p_{D_j}}{\partial t_D}G_{D_j}(r_D,r'_D,t_D,t'_D),\ dt'_D dr'_D\right)=1 \tag{85}$$

Denominating the solution for pseudo pressure in the well by m_{w_D} the pseudo-pressure Coupling Condition allow us to use:

$$m_{w_D}(t_D)=m_{D_1}(r_D=1,t_D)=m_{D_2}(r_D=1,t_D)=\ldots = m_{D_n}(r_D=1,t_D) \tag{86}$$

So, replacing Eq. (86) in Eq. (85) and rearranging the terms, the well pseudo-pressure solution is given by:

$$m_{w_D}(t_D)=p_D(t_D)-\frac{2\pi}{h_T}\sum_{i=1}^{n}h_j\int_0^{\infty}\times\int_0^{t_D} r'_D w_{D_j}(p_{D_j})\frac{\partial p_{D_j}}{\partial t_D}G_{D_j}(r_D,r'_D,t_D,t'_D)\ dt'_D\ dr'_D \tag{87}$$

3. Material and methods

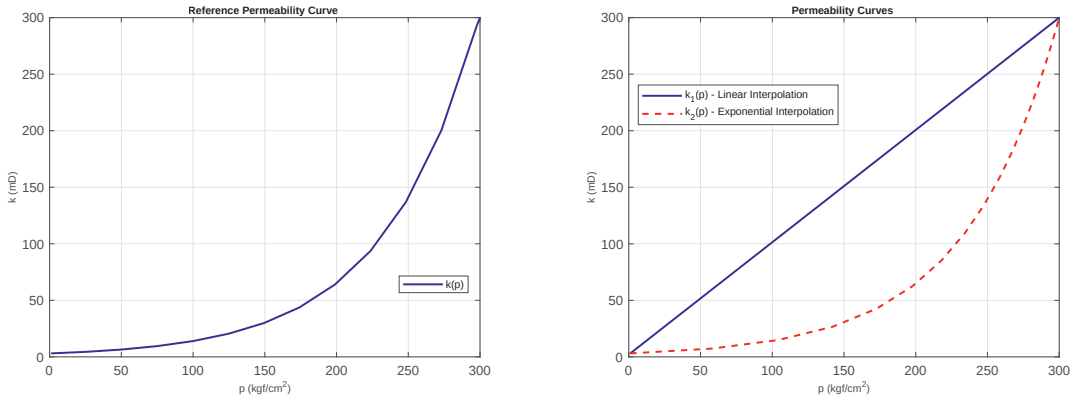
This section discusses the numerical methods used to compare the results obtained from the presented model with a commercial flow simulator, considering different scenarios of a two-layer reservoir.

3.1. Flow-rate approach and permeability curves

In the proposed formulation, it is necessary to use the wellbore flow rate in each layer. For this, we use a methodology that can approximate this flow rate considering an equivalent one-layer reservoir and using Darcy's Law:

$$q_j\approx\frac{2\pi q k_j(p_i)}{k_{eq}(p_i)h_t} \tag{88}$$

Despite that, the model requires a permeability function to calculate the response of the pseudo-pressure. Fernandes (2022)



(a) Reference Permeability Curve (b) Interpolated Permeability Curve

Fig. 2. Permeability curves.

used a permeability curve from a label experiment of the pressure-dependent permeability show in Fig. 2(a).

It is possible to perform a linear and exponential interpolation to estimate permeability values to fit new points. Fig. 2(b) shows examples of the interpolations based on the permeability curve of Fig. 2(a).

3.2. Computacional aspects

For the numerical calculations presented in this section, measurements were compatible with the Brazilian system. Therefore, the adequacy constants for pressure measurements over time were coupled to the equations presented in Section 2:

$$t_D = \alpha_t \frac{k_{eq}(p_i)}{\phi \mu c_t r_w^2} t \tag{89}$$

and

$$m_{w_D}(t_D) = p_D(t_D) - \frac{\alpha_p}{h_T} \sum_{i=1}^{n} h_j \int_0^{\infty} \times \int_0^{t_D} r'_D w_{D_j}(p_{D_j}) \frac{\partial p_{D_j}}{\partial t_D} G_{D_j}(r_D, r'_D, t_D, t'_D) dt'_D dr'_D \tag{90}$$

where $\alpha_t = 0.0003484$ and $\alpha_p = 19.03$ are adequacy constants for Brazilian measurements.

The proposed model is solved through a computational code developed in MATLAB. The source line solution, expressed by the exponential integral function $Ei(r_D, t_D)$, is computed through the command $expint(t_D)$ in the MATLAB scientific library. The following pseudo-code in MATLAB software implements the proposed solution. This algorithm provides graphs of the pseudo-pressure response against the source line response. The analysis of the graphs obtained will be discussed below.

Algorithm 1. Pseudo-pressure Model Solution

1: Input the reservoir initial data (q, h_j, $k_j(p_i)$, μ, ϕ, ...)
2: Discretize radius and time steps (r, t)
3: Compute variables dimensionless (r_D, t_D)
4: **for** each time step **do**
5: Compute the experimental ith term of $(p_{D_j}, k_{D_j}(p_{D_j}), H_{D_j}, w_{D_j})$
6: Compute the ith term of the approximated layer flow rate (q_j) and ith term C_j
7: Compute the zero-order terms $m^0_{D_j}$ by Eq. (77)
8: Compute the first-order terms $m^1_{D_j}$ numerically by Eq. (78)
9: Compute the dimensionless well pseudo-pressure response m_{wD} like Eq. (79)
10: **end for**
11: Plot graphs

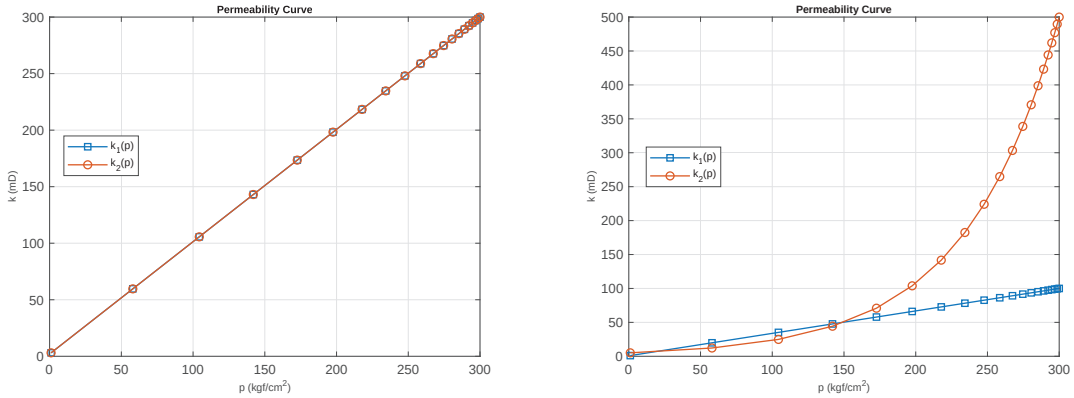
Some mathematics methods were used to help the numerical computation: The experimental terms were obtained by performing a linear or exponential interpolation from a database table. The double integral to compute the first-order term $m^{(1)}_{D_j}(r_D, t_D)$ was calculated using the Gaussian Quadrature Method for double integral. The pseudo-pressure derivative was calculated using the analytical expression of the derivative source-line solution.

4. Results

In oil production tests, reservoir characterization needs a variety of physical parameters that have a direct impact on well performance and the interpretation of the data. For instance, fluid viscosity plays a key role in controlling flow resistance, while the compressibility of the oil is fundamental to understanding how the system responds to changes in pressure. In this study, we consider an initial reservoir pressure (p_i) of 300 (kgf/cm^2) as the baseline from which the pressure declines during production begins. The flow rate is another important operational parameter widely used to evaluate well behavior. For analytical purposes, it is common to

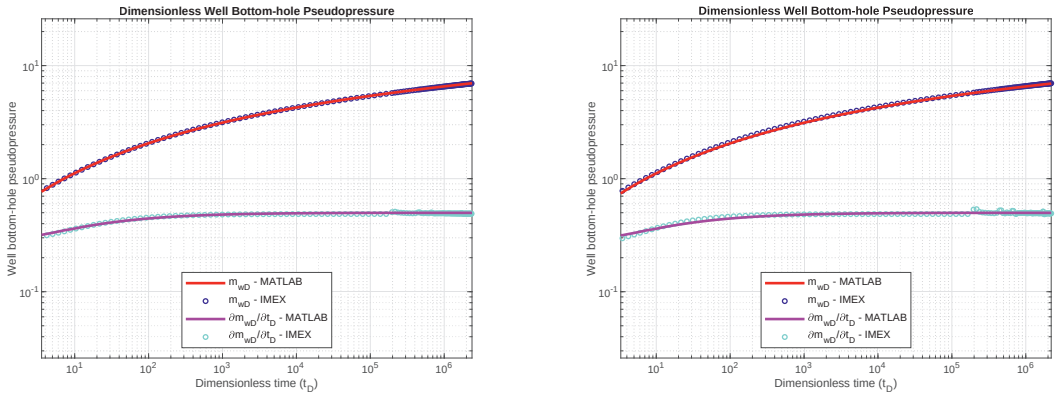
Table 1
Reservoir properties.

Case	r_w (m)	q (m^3/day)	Layer	$k_j(p_i)$ (md)	$k_{eq}(p_i)$ (mD)	Permeability Curve Type	ϕ	μ (cp)	h_j (m)	c_t $(kgf/cm^2)^{-1}$
A1	0.1	500	1 and 2	300	300	Linear	0.3	5.0	45	2.5×10^{-5}
A2	0.1	2000	1 and 2	300	300	Linear	0.3	5.0	45	2.5×10^{-5}
B1	0.1	500	1	100	300	Linear	0.3	5.0	45	2.5×10^{-5}
			2	500		Exponential	0.3	5.0	45	
B2	0.1	2000	1	100	300	Linear	0.3	5.0	45	2.5×10^{-5}
			2	500		Exponential	0.3	5.0	45	



(a) Cases A1 and A2 (b) Cases B1 and B2

Fig. 3. Permeability curves cases A and B.

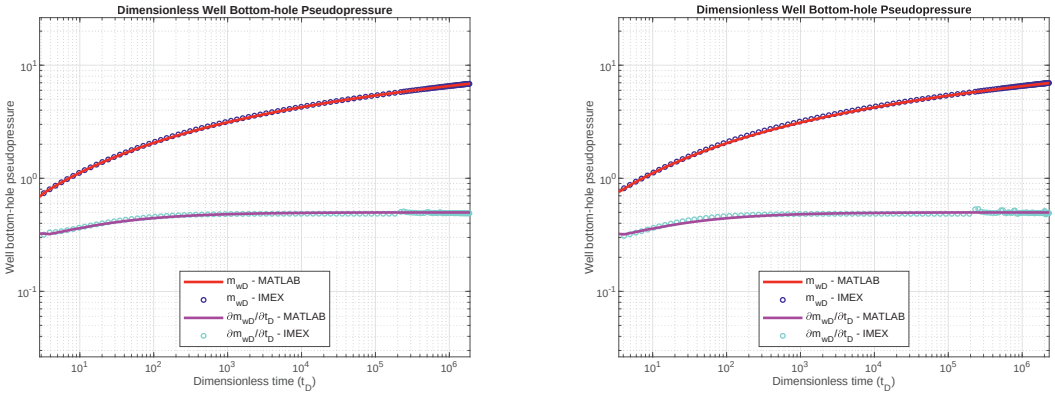


(a) Case A1 (b) Case A2

Fig. 4. Cases A: loglog of pseudo-pressure and its derivative.

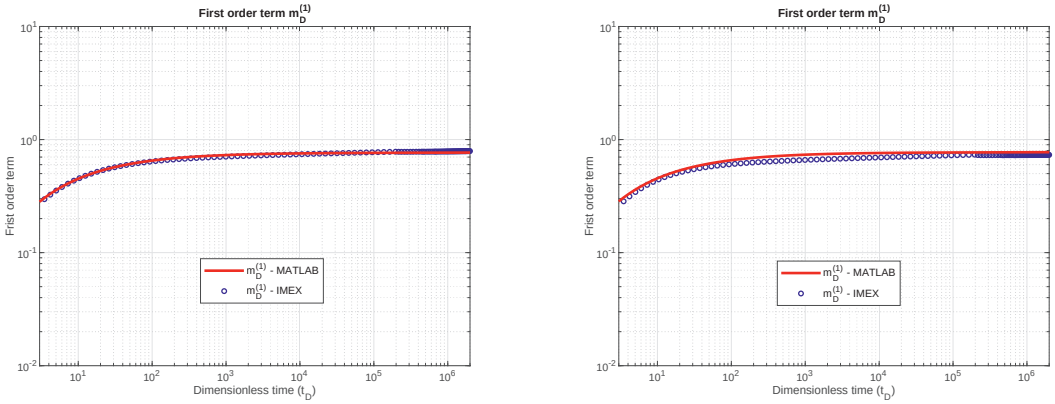
work with reference values between 80 and 800 m^3/day, though these are adjusted based on the well's actual capacity and operational limitations. In the results presented here, we explore two scenarios: one with a flow rate close to the standard range and another with a substantially higher flow rate. This approach enables us to understand better how various operational conditions impact the reservoir's response. Permeability is also an important property, often measured in millidarcy (mD), which provides insight into the quality of the reservoir. Typically, productive formations have permeabilities above 100 mD, but tests can also involve low-permeability rocks. The goal of this section is to analyze the impact of the permeability variation as a function of pressure in different scenarios. Permeability may decrease significantly as pressure drops, which can severely limit flow and reduce long-term productivity. By carefully evaluating these factors, we can anticipate challenges such as formation damage or rock compaction. This deeper understanding is essential for building more accurate predictive models and, ultimately, for designing more effective and sustainable production strategies.

In this section, we analyze the pseudo-pressure response compared to the results obtained from the commercial simulator IMEX. This simulator calculates the pressure response in the well using the finite difference method for each time step. For comparison purposes, the pressure results from the simulator are adjusted to an equivalent pseudo-pressure curve. The graphs to be analyzed refer to the log-log scale, which facilitates understanding



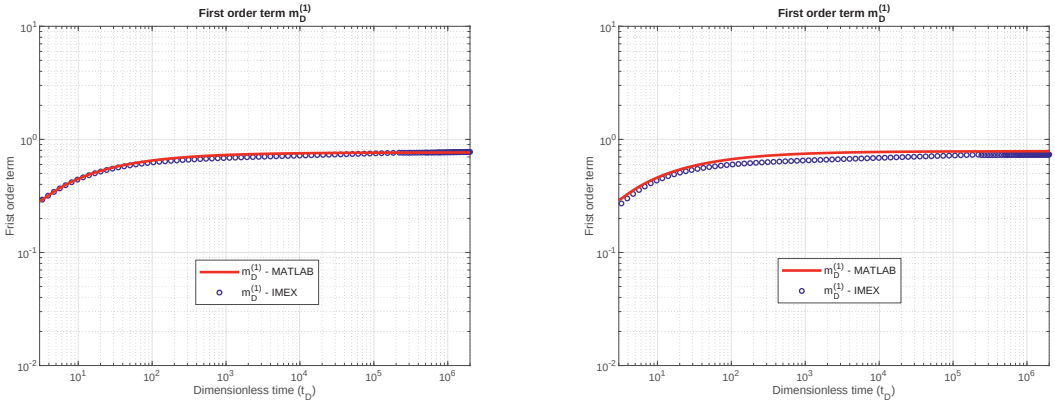
(a) Case B1 (b) Case B2

Fig. 5. Cases B: loglog of pseudo-pressure and its derivative.



(a) Case A1 (b) Case A2

Fig. 6. Cases A: first-order term.

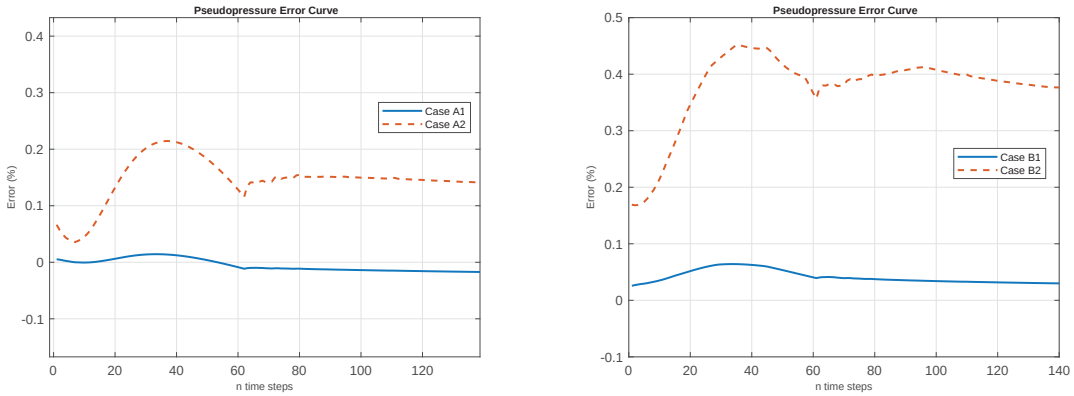


(a) Case B1 (b) Case B2

Fig. 7. Cases B: first-order term.

of the pseudo-pressure behavior. This representation also aids in comparing our model with obtained data by the flow simulator, improving the accuracy of reservoir characterization (Samaniego et al., 1977; Tabatabaie et al., 2015). Additionally, the derivative graphs presented in this section are based on the Bourdet derivative (Bourdet et al., 1989). In all cases to be discussed, a two-layer reservoir will be considered, and the properties applied in Cases A and B scenarios are presented in Table 1.

Note that the cases differ only in the permeability curves for each layer. In Case A, linear and identical permeability curves are



(a) Error Curve Cases A1 and A2

(b) Error Curve Cases B1 and B2

Fig. 8. Pseudo-pressure errors.

considered for each reservoir layer, while Case B uses two different permeability curves for each layer: linear and exponential. The permeability curves used in Cases A and B are shown in Fig. 3(a) and (b), respectively.

Fig. 4(a) and (b) show the pseudo-pressure data for Cases A1 and A2, respectively, along with their derivative curves.

Recall that these cases differ in the flow rate used, but both assume equal linear permeability curves. The graphs show excellent agreement between the obtained responses. The temporal derivative curves indicate that, at early times, the permeability curve influences the result. In contrast, the temporal derivative curve represents a constant slope for a classical model with constant permeability.

Cases B1 and B2 also differ in the flow-rate used. In Fig. 5(a) and (b) we observed good agreement between the obtained responses for Cases B1 and B2. The exponential permeability curve influences the pseudo-pressure response more than the linear permeability curve.

It was shown that the solution proposed in this work consists of two terms sum (Eq. (87)): the zero-order term, which corresponds to the classical solution for constant permeability, and the first-order term. It is interesting to analyze the behavior of the first-order term curves because this is a corrective term of the classical solution. The flow simulator's first-order term can be constructed using the reference table of pressure-pseudo-pressure values. So, the numerical response relative to the first-order term associated with the flow simulator can be found by the pressure response interpolation. In this work, the interpolation chosen was the Newton interpolation. Fig. 6(a) until 7(b) shows the first-order term behavior compared to the IMEX response.

All the curves exhibited good similarity. It is possible to observe that the difference between the curves relating to a higher production flow is more pronounced in the curves relating to a higher production flow. However, despite this small order difference, the behavior of the curves remains similar.

Fig. 7(a) and (b) show that cases B1 and B2 are more pronounced than cases A, which are more straightforward. This can be explained by the fact that, in this case, an exponential curve is used. Therefore, the simulator's numerical calculations become more complex, which may represent a disadvantage associated with loss during interpolation to obtain the first-order term. Despite that, all the curves presented show a good agreement between the behavior of the proposed analytical solution and the solution obtained using the flow simulator.

Due to internal policy issues and the fact that this work was part of a university research project, it was impossible to access real data. Therefore, a metric was created to analyze the difference between the responses obtained by the presented work and the flow simulator. Considering the IMEX response as a reference, it was possible to calculate the percentage error between the solutions for each time step:

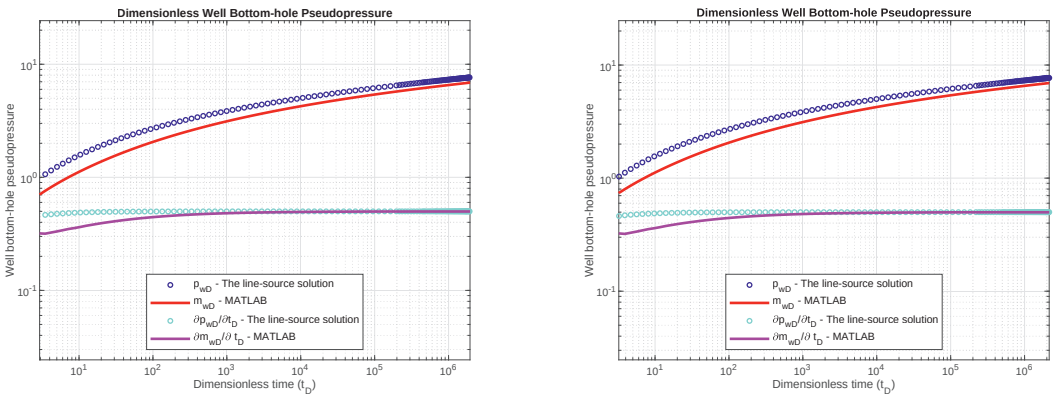
$$error = 100\frac{(m_{wD_{MATLAB}} - m_{wD_{IMEX}})}{m_{wD_{IMEX}}} \tag{91}$$

The differences observed in graphs Figs. 4 and 5 for the initial times become more evident in the error graph represented by Fig. 8(a) and (b). This difference occurs due to the more significant influence of pressure-dependent permeability at the initial times. For the high flow rates used in Cases A2 e B2 (Fig. 4(b) and 5 (b)), the response of the flow simulator becomes less accurate, but they still have similar behavior to the presented model. Since different methods calculate the response in each model, it is more likely that a more substantial difference will occur between the responses obtained in the initial period. It is possible to observe that the error is minor and tends to be a constant value for longer times in all cases. This difference occurs because, for a long time step, the influence of permeability as a function of pressure decreases, thus causing the responses of both models to approach the classical solution of single-phase flow with constant permeability. This fact is evidenced by the response of the derivatives curves, which tend to have a constant value. Despite all these factors, the errors obtained were less than 1% for all points, thus showing a good similarity between the solutions.

5. Discussions

In oil and gas production, pseudo-pressure models are essential for well deliverability, optimizing production strategies, and enhancing the accuracy of reservoir simulations (Bourdet et al., 1989). Research into the relationship between permeability and pressure is essential for improving reservoir management and optimizing extraction processes. By employing these formulations, we can develop more precise reservoir simulation models.

This work proposes a solution for a permeability-dependent pseudo-pressure model designed for multilayered reservoirs, showcasing results specifically for two-layer reservoirs. While similar studies have explored various types of pseudo-pressure, to the authors' knowledge, the solutions developed in this research



(a) Case A1 (b) Case B1

Fig. 9. Comparison between Source line Solution and Pseudo-Pressure model.

have not previously addressed multilayered reservoirs with this level of detail. The computational performance of the proposed models achieved a good match with flow simulators, hence justifying the model and realizing the authors' objectives. Furthermore, flexibility in the model allows for experimentation with varying conditions, e.g., reservoirs characterized by a higher number of layers, different fluid and rock properties, and different permeability-pressure relations. Such versatility renders the model quite effective as a reservoir management and optimization tool.

5.1. Comparison with line-source solution

The comparison of the line-source solution for flow with constant permeability to our analytical model that considers permeability as a function of pressure is an essential analysis for an assessment of reservoir behavior. In porous media where permeability exhibits a pressure dependence, such as highly compactable formations or naturally fractured reservoirs, neglecting this variability can lead to inaccuracies in flow predictions. A systematic evaluation of the discrepancies between these models enables more precise quantification of permeability effects on single-phase flow, improving the reliability of production forecasts.

The source line solution is a classic analytical tool widely used in reservoir engineering to model fluid flow in porous media, including the case of single-phase oil flow in a reservoir with multiple layers. Even with the advancement of complex numerical simulators, the source line solution still serves as a theoretical reference and validation of numerical models, especially in pressure tests. The source line solution assumes as a hypothesis that permeability is constant. Therefore, it serves as a fundamental analytical reference to compare and evaluate complex models, such as those in which permeability varies with pressure. This comparison is essential because it allows identifying the real impact of nonlinearity on flow behavior, isolating the effects of permeability variation on pressure distribution and well productivity.

Fig. 9(a) and (b) shows the result obtained for Case A1 and B1 regarding the pseudopressure and its logarithmic derivative in direct comparison with the response of the Source Line Solution.

The graph analysis allows us to conclude that the influence of the pressure-dependent permeability curve occurs at the initial times. It is also possible to observe that the derivative curve resembles the homogeneous case for a long time.

5.2. Applications in reservoir exploration and development

The findings reported here have several implications for practice. The suggested model can be utilized to develop production strategies for multilayer reservoirs, particularly unconventional reservoirs with severe pressure-dependent permeability effects. By enhancing reservoir performance forecasts, operators can optimize recovery rates and simultaneously minimize risks and operating costs. The model could be a real-time reservoir monitoring system platform, whereby permeability variations related to pressure dependencies may lead to production level adjustments or the implementation of enhanced oil recovery methods.

During the reservoir exploration, laboratory tests help determine the economic potential for the reservoir's oil production. These tests are powerful tools for estimating rock properties, such as the permeability curve. However, they are expensive due to the need for sophisticated equipment. They can also change the properties of the rock sample since, during extraction, the original properties can be altered due to effects such as depressurization and loss of native fluids, or they can even cause the sample to become unusable during the test. Given these limitations, the model presented can be used as an alternative solution for this type of low-cost measurement.

Also, the presented model can be used as a basis for applying the inverse problem, allowing the calibration and validation of the model based on accurate data, ensuring greater accuracy and reliability in the predictions. Since reservoir parameters, such as permeability and porosity, cannot be measured directly throughout their entire length, the solution of the inverse problem makes it possible to estimate these values based on observations of pressure and flow in the wells. In this way, our numerical model can be adjusted to better represent the reservoir's behavior reducing uncertainties and assisting in strategic decision-making for exploration and production development. Furthermore, integrating the inverse problem into the developed model increases its practical applicability, allowing it to optimize reservoir management in real scenarios.

Although it demonstrated good equivalence with the flow simulator for the cases presented, since it is a numerical model, it should be noted that the model may not perform with the same precision for more complex permeability curves. In addition, the model uses some simplifying assumptions which apply to particular cases. However, the mathematical model can be extended to consider more complex assumptions in future work.

6. Conclusions

The geometry of a reservoir directly influences the application of Green's Function in fluid flow problems, especially in the mathematical modeling of pressure and permeability in oil and gas reservoirs.

The Green's function plays a significant role in modeling fluid flow in oil reservoirs, and its relationship with the reservoir geometry is direct and fundamental. The Green's function in this context represents the response of the pressure system to a point injection of fluid. This characteristic is advantageous because it allows the solution to be constructed through superposition for any source (well) configuration. Therefore, for similar or more complex problems, Green's function can be adapted to the reservoir geometry.

Although there are different studies in the literature that use similar geometries, to the authors' knowledge, no methodologies have been identified for the application of this method to reservoirs with multiple layers. Therefore, this work is a significant contribution that may be a precursor to new, more complex models that use a similar methodology since infinite homogeneous reservoirs have more straightforward solutions. In contrast, bounded or fractured reservoirs require more complicated adjustments.

As this research has demonstrated, incorporating pressure-dependent permeability behavior into reservoir engineering models can lead to more reliable predictions of production rates. This advancement enables more efficient reservoir management, better resource allocation, and enhanced sustainability in hydrocarbon extraction, ultimately supporting the development of innovative approaches in reservoir engineering. Since this is an academic study, the most significant limitation of the results presented in this article is the lack of access to accurate data to test the model's applicability to real situations. In addition, using different numerical methods during the model implementation may result in a greater margin of error depending on the complexity of the permeability curve used.

In future work, we plan to expand this formulation to include heterogeneous reservoirs composed of two or more homogeneous regions with pressure-dependent permeability. Numerical methods will be implemented to improve the precision of the solutions, aligning them with the proposed methodology. These enhancements will further support complex reservoir modeling, offering a broader range of applications in the oil and gas industry, including optimized reservoir simulation workflows and improved forecasts for long-term field performance.

CRediT authorship contribution statement

Jessica Lailla Ferreira Bittencourt Neto: Writing – original draft, Visualization, Validation, Software, Methodology, Investigation, Formal analysis, Conceptualization. **Sinésio Pesco:** Supervision, Project administration, Methodology, Formal analysis, Conceptualization. **Abelardo Borges Barreto Júnior:** Supervision, Project administration, Methodology, Formal analysis, Conceptualization.

Declaration of competing interest

The authors declare that they have no known competing financial interests or personal relationships that could have appeared to influence the work reported in this paper.

Acknowledgements

This study was financed in part by the Coordenação de Aperfeiçoamento de Pessoal de Nível Superior - Brasil (CAPES) - Finance Code 001. Authors are grateful to Petrobras for partially sponsoring this research.

References

Barreto, A.B., 2011. Nonlinear gas well test problems: a generalized perturbative solution applied to a vertical well near a sealing fault. In: Proceedings of the 2011 SPE Annual Technical Conference and Exhibition.

Barreto, A.B., Pires, A.P., Peres, A.M., 2012. A new rigorous analytical solution for a vertical fractured well in gas reservoirs. In: Proceedings of the 2012 SPE Latin America and Caribbean Petroleum Engineering Conference.

Barreto, A.B., Peres, A.M.M., Pires, A.P., 2013. A variable-rate solution to the nonlinear diffusivity gas equation by use of green's-function method. SPE J. 18, 57–68.

Bittencourt Neto, L.F., Bela, R.V., Pesco, S., Barreto, A., 2020. Laplace domain pressure behavior solution for multilayered composite reservoirs. In: Proceedings of the 2020 SPE Latin American and Caribbean Petroleum Engineering Conference.

Bourdet, D., 1985. Pressure behavior of layered reservoirs with crossflow. In: Proceedings of the 1985 SPE California Regional Meeting.

Bourdet, D., Ayoub, J.A., Plrard, Y.M., 1989. Use of pressure derivative in well test interpretation. SPE Form. Eval. 4, 293–302.

Chen, Z., Huan, G., Ma, Y., 2006. Computational Methods for Multiphase Flows in Porous Media. Society for Industrial and Applied Mathematics (SIAM), 978-0-89871-613-3.

Civan, F., 2016. Reservoir Formation Damage: Fundamentals, Modeling, Assessment, and Mitigation, third ed. Gulf Professional Publishing. 978-0-12-801898-9.

dos Santos Sousa, E.P., 2014. Gas well testing with wellbore storage and skin: a line source solution using the Green's functions approach. In: Proceedings of the 2014 SPE Annual Technical Conference and Exhibition, Amsterdam, The Netherlands.

Duff, D.G., 2001. Green's Functions with Applications. Chapman and Hall/CRC.

Duong, A.N., 1989. A new set of type curves for well-test interpretation with the pressure/pressure-derivative ratio. SPE Form. Eval. 4 (2), 264–272.

Fernandes, F.B., 2022. Perturbative-integro-differential solution for the nonlinear hydraulic diffusivity equation for infinite-acting-oil flow in a permeability-pressure-sensitive reservoir. SPE Reservoir Eval. Eng. 25, 530–567.

Fernandes, F.B., Braga, A.M.B., Soares, A.C., Rezende, F.H.G., 2023a. Perturbative-integro-differential solution for the nonlinear hydraulic diffusivity equation for compaction damage management in poroelastic stress-sensitive oil reservoirs. In: Proceedings of the 2023 Offshore Technology Conference Brasil.

Fernandes, F.B., Braga, A.M.B., de Souza, A.L.S., Soares, A.C., 2023b. Analytical solution of the nonlinear hydraulic diffusivity equation with depletion-dependent permeability in oil wells near sealing faults. Transport Porous Media 148, 215–244.

Fernandes, F.B., Braga, A.M.B., Duarte, M.C., Rezende, F.H.G., 2025. Reservoir production forecast with depletion-dependent rock-fluid properties using a poroelastic dupuit's formula. In: Proceedings of the 59th US Rock Mechanics/Geomechanics Symposium. New Mexico, Santa Fe.

Gringarten, A.C., Ramey Jr., H.J., 1973. The use of source and Green's functions in solving unsteady-flow problems in reservoirs. Soc. Pet. Eng. J. 13 (5), 285–296.

Lee, J., Wattenbarger, R.A., 2016. Gas Reservoir Engineering. Henry L. Doherty Memorial Fund of AIME. Society of Petroleum Engineers.

Miranda, F.A., Barreto, A.B., Peres, A.M., 2016. A novel uniform-flux solution based on the Green's function method for modeling the pressure-transient behavior of a restricted-entry well in anisotropic gas reservoirs. SPE J. 21, 1870–1882.

Neto, A.C.L., 2019. Modelagem Matemática de Teste de Pressão em Reservatórios de Gás com Região de Permeabilidade Reduzida em Torno dos Poços. Centro de Ciências e Tecnologia, Universidade Estadual do Norte Fluminense, Rio de Janeiro. MSc Dissertation.

Raghavan, R., Scorer, J.D.T., Miller, F.G., 1972. An investigation by numerical methods of the effect of pressure-dependent rock and fluid properties on well flow tests. Soc. Pet. Eng. J. 12 (3), 267–275.

Raghavan, R., 1993. Well Test Analysis. Prentice Hall.

Ramey Jr., H.J., 1966. Application of the line source solution to flow in porous media — a review. In: Proceedings of the SPE-AIChE Joint Symposium.

Samaniego, V.,F., Brigham, W.E., Miller, F.G., 1977. An investigation of transient flow of reservoir fluids considering pressure-dependent rock and fluid properties. Soc. Pet. Eng. J. 17 (2), 141–150.

Singh, K., Whitson, C.H., 2010. Gas-condensate pseudopressure in layered reservoirs. SPE Reserv. Eval. Eng. 13 (2), 203–213.

Sousa, E.P., Barreto, A.B., Peres, A.M., 2015. Finite-wellbore-radius solution for gas wells by Green's functions. SPE J. 20, 842–855.

Sousa, E.P., Barreto, A.B., Peres, A.M., 2016. Analytical treatment of pressure-transient solutions for gas wells with wellbore storage and skin effects by the Green's functions method. SPE J. 21, 1858–1869.

Tabatabaie, S.H., Pooladi-Darvish, M., Mattar, L., 2015. Draw-down management leads to better productivity in reservoirs with pressure-dependent permeability — or does it?. In: Proceedings of the 2015 SPE Canada Unconventional Resources Conference.

Van Everdingen, A.F., Hurst, W., 1949. The application of the laplace transformation to flow problems in reservoirs. J. Pet. Technol. 1, 305–324.

Wang, J., 2023. Gas/water transient rate analysis and parameters evaluation by integrating pseudopressure-based approach with deep-learning method. In: Proceedings of the 2023 SPE/IATMI Asia Pacific Oil & Gas Conference and Exhibition, Jakarta.